OVERVIEW OF RECENT STUDIES AT IPST ON CORRUGATED BOARD EDGE COMPRESSION STRENGTH: TESTING METHODS AND EFFECTS OF INTERFLUTE BUCKLING

Roman E. Popil

Several recent series of investigations were conducted on corrugated board performance in the areas of: loaded container endurance in cyclic humidity, predictive models for edge compression strength (ECT), effects of lightweight facings, measurement of transverse shear rigidity, effects of adhesive level, and out-of-plane crushing on ECT. The course of this program prompted exploration and review of several aspects of ECT testing methods: specimen height, test duration, and fixture-clamping effects. In this review, ECT values are shown to be influenced by the combination of the selected testing technique with the specific structural and strength characteristics of the board being tested. The effect of specimen height on selected single wall C-, E-, F-, and N-flute boards is measured and rationalized using a simplified beam-theory approach. Apparent loss of ECT in a C-flute crushed board is explored to determine whether mitigation is possible by selection or modification of testing method. Investigations of platen speed effects on C-flute substantiate previous work. Lightweight facings on A- and C-flute corrugated boards are observed to display localized buckling, which affects the ECT value. An analytical model that combines the measured bending stiffness of the facings and the compression strengths of the fluting and facings provides an improved predictive accuracy and is applied to a series of laboratory and commercial corrugated boards.

Keywords: Compression testing; Corrugated board; Linerboard; Testing methods; Mechanics; Bending stiffness

*Contact information: Georgia Institute of Technology, Institute of Paper Science and Technology (IPST) 500 10th St NW, Atlanta, Georgia 30332 USA; * Corresponding author: Roman@gatech.edu*

INTRODUCTION

The edge compression strength of corrugated board (ECT TAPPI Methods 811, 838, 839) is routinely used as a primary measure of shipping container board quality. Many box-making operations rely on this seemingly simple compression-to-failure test to optimize their processes such as selection of components, adhesive application level, process moisture levels, etc. The test essentially consists of placing a prepared sample of corrugated board on its edge between parallel platens, one of which traverses towards the other and is connected to a load cell. Deformation of the board progresses until the board fails at few percent strain by the formation of an out-of-plane folding crease, and there is a corresponding fall in recorded platen load. Some confusion arises from the availability of several different methods with varying claims of accuracy or applicability. The increasing market prevalence and trend toward lighter basis weight corrugated board

products often present lower than expected ECT values based on component strength properties. The question of the testing method affecting results arises in these cases. An optimal measure of ECT for a given type of corrugated board would provide the maximum possible value reflecting the compression strength of that corrugated board, uncompromised by testing artifacts. A reliable ECT measurement is desired to ensure that a minimum basis weight of fiber is utilized in production to achieve a given strength target. The tester is challenged to select the method that is best suited for the particular board in production.

An industry consortium funded program at IPST (now known as the Institute of Paper Science and Technology at Georgia Tech, Atlanta, Georgia, USA) was directed to determine strategies to maximize corrugated container performance at reduced basis weight. During the course of these investigations, several questions arose from the industry participants regarding the sensitivity of compression strength measurement to: a) the type of method, b) sample preparation, c) the effect of crushing, and d) the effect of test duration. The research program investigated corrugated box performance through the preparation of various corrugated boards of varying basis weights and configurations using the available pilot corrugating facilities (Popil *et al*. 2004; Popil 2005; Popil and Schaepe 2005; Schaepe and Popil 2006; Popil *et al*. 2006; Haj-Ali *et al*. 2008; Popil and Hojattie 2008; Popil 2010).

These investigations showed in several circumstances that ECT values deviated from predictive models, depending on the board structure tested and the selected testing method. In particular, boards prepared with lightweight medium or those that have been subjected to out-of-plane crushing require special attention to test method. Board samples used in a series of creep behavior studies were of slightly differing dimensions compared to those used in standardized ECT, so the sensitivity of ECT to specimen height required quantification to validate the results. Some instruments used in the research were set by default to slightly differing platen travel speeds; therefore the effect of test duration on ECT was determined as well. Therefore, ECT methods and parameters were explored extensively to qualify the results reported in the research program. As a result, the dependence of ECT on test specimen height and platen speeds were characterized for some selected boards, leading to a confirmation of some previous observations and recommendations for optimal testing methods are presented in this paper.

Test samples subjected to ECT are often observed to undergo a characteristic patterned buckling of the facings prior to reaching the peak failure load at which a crease forms with a simultaneous decrease in platen load. In these cases, the buckling load of the facing panels contained between consecutive glue lines is less than the compression strength, which allows the facings to buckle prior to compression failure. Thus, the failure mechanism here can be considered to be similar to BCT (box compression strength) consisting of combined compression and bending failure. Combining compression and bending strengths of the facings provides a useful predictive model for ECT similar to BCT with improved accuracy. A combined series of laboratory-made and commercial corrugated boards were investigated for ECT using this combined compression strength and bending resistance model.

Edge Compression Strength Test Methods

All testing methods for ECT generally consist of a corrugated board specimen of prescribed specific dimensions being placed and supported on edge between advancing parallel platens. The load direction is parallel to the flutes or the cross direction (CD) of the board in emulation of the loading direction of assembled corrugated boxes. The peak load sustained prior to specimen failure is recorded as the ECT value in units of force per unit length. The ideal failure that validates a good test is observed to be a crease in the linerboard facings running along the horizontal length of the test specimen away from the horizontal edges. This measure of the strength of corrugated board is the dominant factor predicting vertical box stacking performance (McKee *et al*. 1963) and box lifetime (Allan 2007).

TAPPI testing methods are periodically reviewed by committee and updated as data become available. Tests to failure, such as ECT, are prone to artifacts and can lead to misleading conclusions. Any flaws in the test specimen or test geometry in a compression to failure test can contribute to misrepresentation of the strength. For example, any degree of specimen bending in an ECT test design will result in a lower value of ECT. Thus, bending must be eliminated through selection of an appropriate test specimen size. Similarly, lack of parallelism in the loading edges across the board width or along the thickness or imprecision in the application of uniaxial vertical load will also result in lower ECT values. What is required in a material property optimization program is a test method that is dominantly influenced by the combined strength of the board components and is not affected by specimen dimensions or preparation. Whether ECT data are aberrant may be judged most easily by comparison of the results with a length-weighted summation calculation of the individual component compression strengths, or by comparison of the data with the predictions of a more sophisticated model.

Previous reviews of the ECT testing methods include: McKee *et al*. (1961), Eriksson (1979), Kroeschel (1984), Bormett (1986), and Koning (1986). Effects of board orientation alignment were reported by McLain and Boitnott (1982). Effects of boxmaking operations on ECT were reviewed by Nordman *et al*. (1978), Kroeschell (1992), and Batelka (1994). Contemporaneously with the IPST program, Wilson and Frank (2009) verified the validity of an ECT measurement for some selected B and E flute boards. Effects of sample preparation, cutting, clamping, specimen length, platen speed, and board crushing have all been addressed in the literature. For example, Urbanik *et al*. (1994), established the effect of waxing the ends of specimens and the required period for subsequent moisture equilibration to maintain valid test results. Some of the issues are reexamined here, being pertinent to the IPST corrugated packaging research program and provide additional insight and review. It is generally recognized that some ECT test methods may not be applicable to some corrugated board varieties, particularly those that are constructed of comparatively lightweight materials or have been subjected to crushing damage. This paper reviews the board edge compression test in attempt to understand the mechanisms that influence the test such as specimen dimensions, test duration, effect of clamping pressure, and effect of lightweight facing buckling.

A widely used form of the test, T 839, is gaining increased usage from its comparative convenience. It entails the use of a 50 x 50 mm test specimen held in a spring-loaded clamping test fixture vertically compressed at a prescribed strain rate. This

method is commonly used in corrugated production operations to routinely monitor quality. Clamp fixtures manufactured by Sumitomo in Japan were examined by IPC (Schrampfer and Whitsitt 1988) who established optimal testing parameters for their sample board sets at the time. Here, sample horizontal vertical edges have to be cut squarely and accurately, and the samples are held at its ends in the clamping fixture that applies some pressure through its spring loaded jaws that span about 2/3 of the test specimen height. This fixture arrangement is intended to prevent any bending of the board. Specimen dimensions are specified to remain invariant, irrespective of the board type being tested. However, boards made with lightweight, easily crushable fluting medium may be affected by the clamp pressure, and small caliper flute boards may be subject to bending. Therefore, the opportunity remains to qualify the test method in these cases.

Although the T 839 clamp fixture method is regarded as expedient, the standard official method prescribed by Rule 41 shipping regulations uses unsupported test specimens with reinforced waxed edges (T 811), and so T 811 has been in longer use. In this case, the specimen heights are precisely specified for the common flute types A, B, C in increments of common convenient inch fractions. Supporting guide blocks are placed on either side of the test specimen to assert perpendicularity or vertical alignment and are to be removed once a force in excess of 22 N is attained. Since the sample is held in less restraint than in method T 839, it is reasonable to expect that T 811 will provide lower ECT values in many cases of corrugated board. The development of the test parameters for T 811 is documented in its TAPPI Method references although establishment of the criteria and specification of limits for specimen heights for the various flute sizes does not appear to be clearly documented. Reference is made to 1957 work done at IPC in Appleton Wisconsin (Kroeschell 1984) but the report is lacking detail. Another cursory data set for A-flute board has been published (McKee 1961) and consists of an ECT versus specimen height or Euler curve. A similar plot referring to European work with different parameters is reproduced in the review by Eriksson (1979). A data set clearly showing the effects of specimen height for various boards for various test methods is desirable.

A comparatively less used form of the compression test involves using prepared specimens having width profiles narrowed at the center, thus concentrating the stress there (T 838). This method avoids issues associated with effects of pressure applying jaws in T 839 and the inconvenience of applying wax to reinforce the edges in method T 811. It may provide the highest ECT value for lightweight boards compared to the other methods. Producing samples with the tapered width profile requires a specialized cutter or a template and circular saw (McKee *et al*. 1961; TAPPI TIP 0308-02; Lorentzen and Wettre). The use of cutters or circular saws may damage lightweight boards. Comparison of methods and their applicability to various varieties of corrugated board remain a topic for investigation (Frank 2003, 2009).

EXPERIMENTAL COMPARISONS OF DIFFERENT TESTING METHODS

The effects of different ECT methods were realized in a study of the effects of fluting basis weight on mechano-sorptive creep (Popil and Hojattie 2010). A series of single-wall A-flute boards were produced using the IPST pilot plant facilities with the

basis weight of the linerboard constant at 205 g/m^2 and the basis weight of the medium ranging from 68.3 to 205 g/m^2. The ECT's of the boards were measured using several different methods, and the results are summarized in Fig. 1.

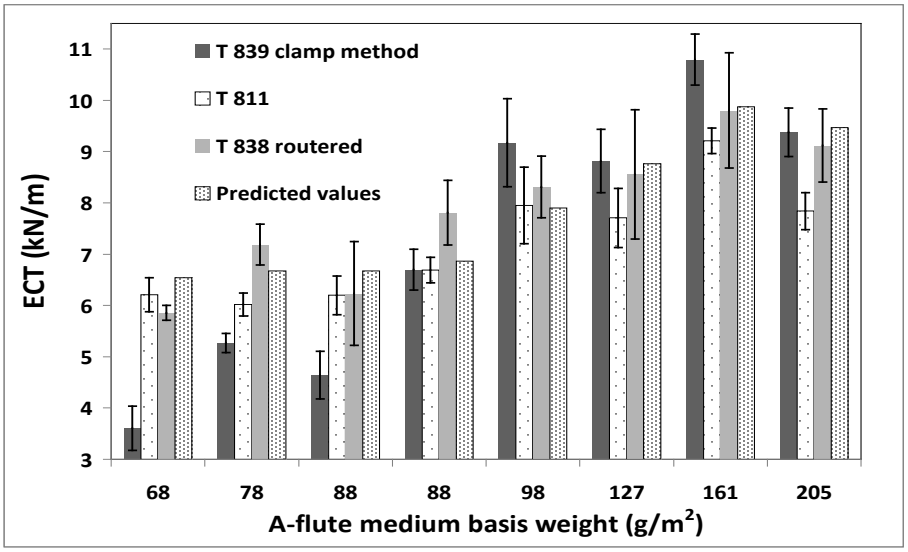

Figure 1. ECT of an A-flute board set using several methods

The results in Fig. 1 can be interpreted using a maximum load equal deformation model (Seth 1985; Dimitrov and Heyndenrych 2009). This assumes the failure mode to be entirely compression at equal strain for all components and is stated as the summation of the length-weighted compression strengths of the components of the single-wall board:

$$ECT \approx 0.7 \times [2(SCT)_l + \alpha (SCT)_m] \quad (1)$$

Here, the compression strengths of the linerboard and medium, $(SCT)_l$ and $(SCT)_m$ respectively, also known as *STFI*, are measured by the short span compression method T 826 and are reported in Popil and Hojjatie (2010). The ratio of fluted medium to linerboard lengths dubbed the take-up factor, is α = 1.42 typically, for most C-flute board. Comparisons can be made with the values of ECT calculated from (1) and actual ECT values obtained from T 811, T 839, and T 838, as shown in Figure 1. Disagreement of actual values from predicted values are largest for T 839 for A-flute boards made with low basis weight medium. The lowest deviation from predicted values overall for this sample set was observed using data from method T 838, so these values were chosen to be used in the analytical model of the effects of board properties on creep behavior.

The T 839 clamp has the effect of pinching the ends of those board samples that have the out-of-plane flat crush resistance lower than the intended typical applied clamping pressure of about 69 kPa. Frank (2004), has indicated that the clamp pressure coming from spring extension is dependent on the caliper of the board, and so may be inappropriate for some lightweight boards of comparatively large caliper. What appears to happen in these cases is that the unclamped facings of the test specimen have a small convex curvature at the onset of increasing load, and the curvature increases to produce a noticeable bending failure rather than compression failure, as shown in Fig. 2. Mechanics

analysis of bowed columns show that buckling load becomes significantly lower (Gere and Timoshenko 1972) and in the case of ECT testing, the bowing leads to an exaggerated bowing/buckling failure.

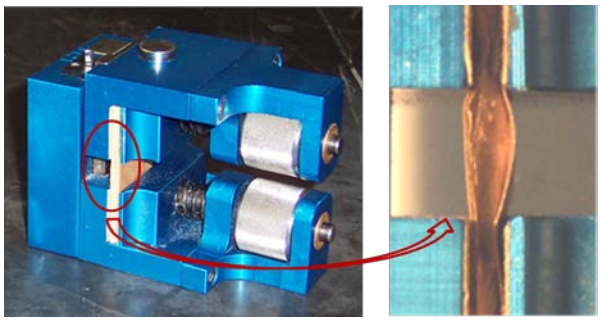

Figure 2. A common version of the T 839 ECT clamp fixture (left) with a close-up (right) of the unclamped region showing the convex bowing of the facings of a previously crushed 112 g/m^2 C-flute corrugated board undergoing vertical compression

BUCKLING/BENDING OF CORRUGATED BOARD

To establish criteria for test specimen height for ECT, beam mechanics is applied to the case of corrugated board in vertical load. Although the strains involved place the compression phenomenon into a non-linear region of elasticity, the simplified approach used here is expected to provide some estimate of the effect of specimen height on ECT. Compression strength is measured convincingly if failure occurs by the formation of a crease and the peak load is not affected by any bending of the test sample. This means that the compressive strength ECT of the test specimen should be less than the buckling load of the test piece. When this condition is fulfilled, the specimen fails by compression and not by bending.

Corrugated board behavior under vertical load can be approximated as a sandwich panel with the structure and the properties of the medium contributing to the flexural rigidity being neglected (Nordstrand 1995; McKee *et al.*1963). The vertically loaded buckling load of a sandwich beam P is considered to consist of a combination of beam buckling P_E and shear P_S (Plantema 1966) expressed as the harmonic mean in the form:

$$\frac{1}{P} = \frac{1}{P_E} + \frac{1}{P_S} \quad (2)$$

The Euler beam buckling load P_E per unit length is $\pi^2 EI/H^2$ or $\pi^2 D_b/H^2$, with I being the second moment of area, H is the height of the vertically loaded beam, and D_b is the beam bending stiffness (or more rigorously, the flexural rigidity once Poisson constants are known). The properties concerned here are the elastic modulus E_{CD} and CD bending stiffness D_{CD}, since the vertical loading in ECT is along the direction of the fluting or cross direction CD. If the ends of the beam are rigidly held or constrained from pivoting, then Euler beam buckling theory predicts the bending load to be $4\pi^2 D_{CD}/H$.

Shear is regarded as significant in (2) based on the following considerations. The shear rigidity P_S for corrugated board has been measured using a torsion pendulum method (Popil *et al*. 2008) for typical C-flute with medium basis weight of 127 g/m^2. Shear rigidity in the CD, designated R_{44}, is 54 kN/m, which is much larger than the corresponding MD value 9.8 kN/m. Buckling loads for typical C-flute samples with D_{CD} of 5 N/m and H in the range of 50 to 32 mm are calculated to be 20 to 48 kN/m, which are comparable to the measured shear rigidity. The validity of approximating the corrugated board as a sandwich structure is reviewed in detail in Appendix A.

A valid ECT measurement for any board must not have bending occurring, which means that the critical buckling load P of that board must be greater that its compression strength ECT. Otherwise, as the compression platens advance and load increases, the board will fail by beam bucking rather than by compression. Upon substitution and rearranging (2) this criterion takes the form,

$$\frac{n^2\pi^2 D_{CD} P_S}{n^2\pi^2 D_{CD} + P_S H^2} \geq ECT \qquad (3)$$

where n = 1 for simple supported ends and n = 2 for the case of rigidly held ends. Equation (3) is used for comparison with experimental data to assess the effect of H on ECT.

EXPERIMENTAL OBSERVATIONS – EFFECT OF TEST SPECIMEN HEIGHT

C-flute board

Two series of parallel experiments were conducted using commercially 42-26C produced board obtained off the corrugator and similar laboratory-produced board using the same components. One series of test specimens had their ends embedded perpendicularly in a quick setting epoxy resin Alumilite™, producing a self-supporting test piece tested in a Universal Testing Machine compression tester, as shown in Fig. 3**.**

Figure 3. An ECT sample embedded in supporting epoxy resin strips front and side views and (right) mounted between the platens of a compression tester

This is a variation of the T 811 method with the horizontal test piece ends encapsulated in hardened epoxy resin platforms instead of being dipped in molten wax. The epoxy

platforms restrict pivoting at the ends and ensure that failure occurs away from the edges in the same manner as in the case of the impregnated hardened wax. This method allows visualization and characterization of any linerboard buckling pattern development that may occur during vertical loading (Popil and Schaepe 2006). Using the platforms eliminates the T 811 requirement for metal supporting blocks that would obscure video recording of the facing behavior during compression.

Preparation of test specimens consisted of cutting samples parallel to the flute direction (CD) to various lengths. These were suspended in a rigid frame support over a machined trough filled to a depth of a few millimeters with the quick-setting epoxy resin. Horizontal edges subjected to vertical loading were always cut using a Billerud cutter with singly beveled parallel blades to ensure clean and square (Schrampfer and Whitsitt 1988) load bearing edges throughout the course of the experiments. Machined metal blocks and leveling bubbles were used throughout the specimen preparation process to ensure parallelism of the platforms with the compression tester platens. Separated test pieces were compression tested in a Model 1122 Instron Universal Testing Machine using Series IX software to record load and deformation at a crosshead velocity of 12.5 mm/min.

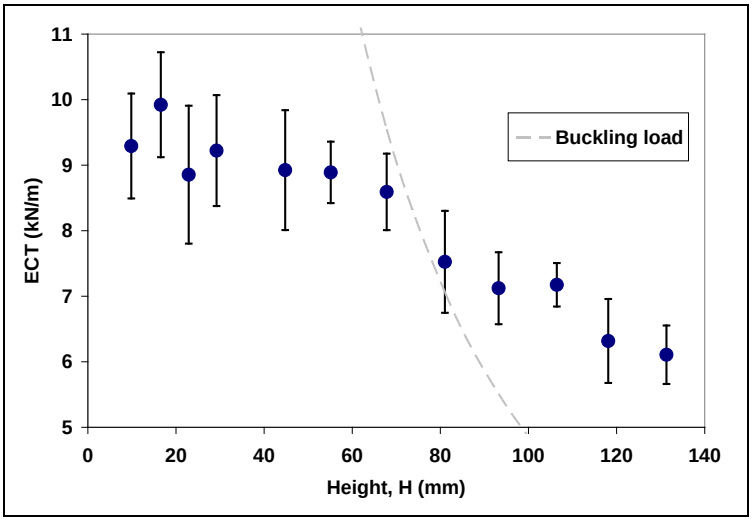

Figure 4. ECT versus the span length for C-flute specimens with the horizontal edges embedded in resin. The dashed curve is the buckling load *P* using Equations (2) and (3), indicating the height above which beam bending is expected to dominate the failure mode.

Figure 4 shows the experimental data for the resin-embedded ends commercial 42-26C C-flute board blank (205 g/m^2 liner, 127 g/m^2 medium single wall) sample set. The data set suggests that the free span between glued ends, *i.e.* a specimen height *H* of up to 80 mm, will provide a constant value of ECT. The fall in ECT value attributable to the onset of beam bending is in general agreement with the estimate provided by beam buckling criterion Equation (3) with n =1. Values for D_{CD} and P_s (R_{44}) for the C-flute board used in (3) are given in Table A1 in the Appendix. The dashed curve in Fig. 4 and in the figures that follow is a plot of Equation (3) with *ECT* set equal to the left hand side term. Loads at a given *H* that are above the curve value are expected to buckle the

specimen. ECT values under the curve value should be representing boards that are failing by compression with no bending. Error bars denote the 95% confidence intervals of 10 repeat measurements at each selected *H*.

An alternate specimen testing arrangement used a Sumitomo T 839 ECT clamp fixture that was modified for various test piece *H*'s by adhering sets of machined aluminum block spacers under the clamp rod bearing supports. This allowed the spacing between the clamping jaws to vary from the default normal setting of 11.2 mm to 110 mm. Similar results for various *H*'s are shown in Fig. 5 using the same commercially produced C-flute board used for Fig. 4.

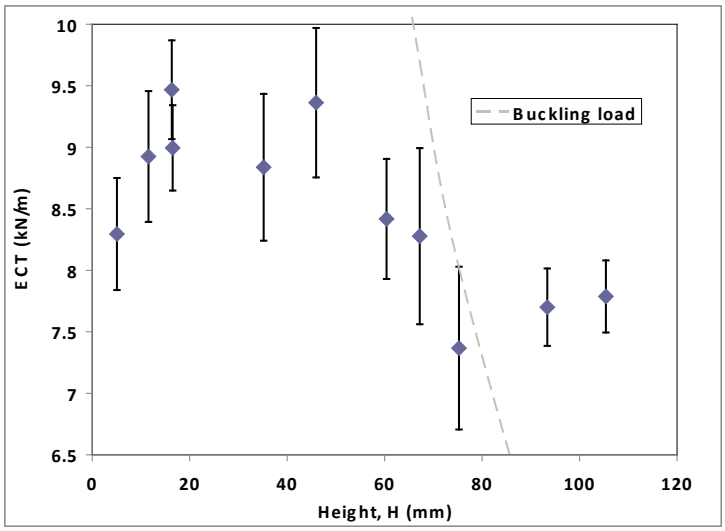

Figure 5. ECT as a function of the free span height for C-flute specimens using a modified Sumitomo clamp to extend the test specimen unclamped height to 110 mm. The dashed curve is the buckling load using the measured bending and shear stiffnesses as in Fig. 4.

The data of Figs. 4 and 5 indicate that a 42-26C test piece height *H* of 60 mm or less ensures an ECT will not be influenced by beam buckling, provided the ends are embedded in resin platforms or are held in the clamp fixture. Throughout this discussion, "free span" is the height *H* of the board that is free of epoxy resin or is not in contact with the jaw faces of the T 839 fixture.

Error bars in the clamped method data shown in Fig. 5 are somewhat higher compared to the resin-embedded end method results shown in Fig. 4. This is likely attributable in part to some degree of compression of the edges in the clamp method versus resin embedded ends and possibly some lack of true parallelism of the clamps with the progressive insertion of machined block assemblies to increase the spacing between the clamps. The expected ECT for this board from (1), is 8.9 kN/m, consistent with the measurements for spans less than 60 mm using both methods. Observations of lower than expected values of ECT at very short *H*'s are reported in McKee (1961) but are likely an artifact.

E-, F-, and N-flute Boards

Compression strength measurements are useful for smaller flute boards to calculate potential stacking strength, as may be need for storage or transport. Mini-flute boards are replacing folding cartons in many applications. There are no accepted standards for compression measurement in this case, so it is useful to qualify a current ECT method for mini-flutes. Samples of commercially made E-, F-, and N-flute board blanks were cut to various lengths and tested in similar fashion as described above for the C-flute board. These boards all had a liner of 207 g/m^2 and fluted medium of basis weight 112 g/m^2.

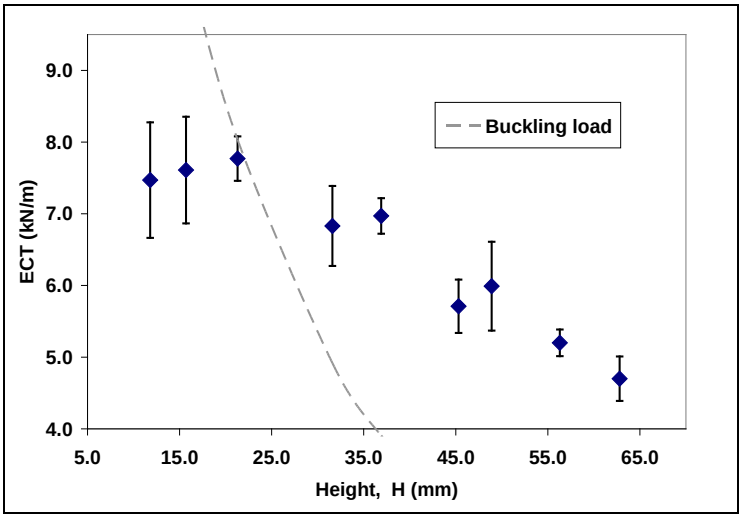

Figure 6. ECT as a function of the free span length for resin embedded edges, E-flute test specimens

Results for resin-embedded edges E-flute specimens are shown in Fig. 6. A fall in ECT occurs with increasing free span *H*, as expected from increased bending at larger *H*. Calculations for the buckling load curve in Fig. 6 is the same as for C-flute but using D_{CD} and P_S values for E-flute from Table A1.

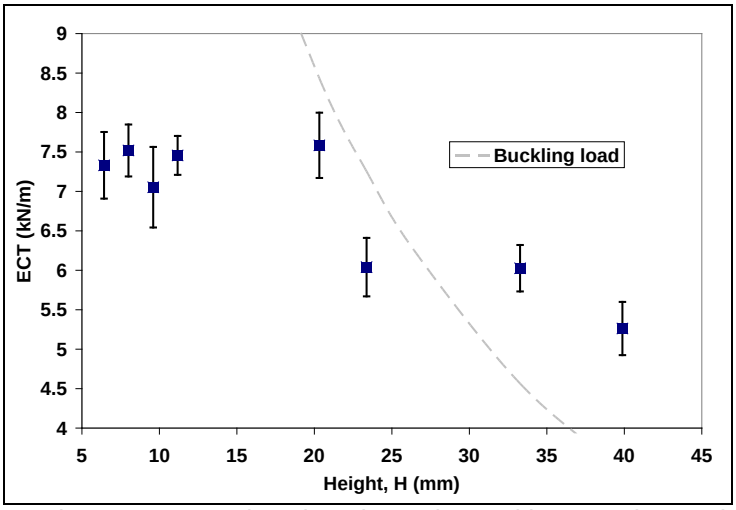

Figure 7. E-flute specimens cut to various lengths and tested in a Sumitomo clamp modified with extensions. The dashed curve is the calculated buckling load.

Figure 7 shows the ECT vs. free span *H* for Sumitomo clamped E-flute board. Figures 6 and 7 suggest that free spans of 25 mm and less will suffice to provide a representative compression strength value for E-flute. The default free span for a 50.8 mm Billerud cut square test piece in the T 839 method is 11.2 mm. Therefore, the T 839 method can be expected to provide a reliable accurate value for this single wall E-flute board.

A similar study was conducted using 42-23F and 42-23N microflute boards using the T 839 clamp only and set to provide various free spans. The data shown in Fig. 8 indicate a plateau in ECT at *H* of 9 mm and less.

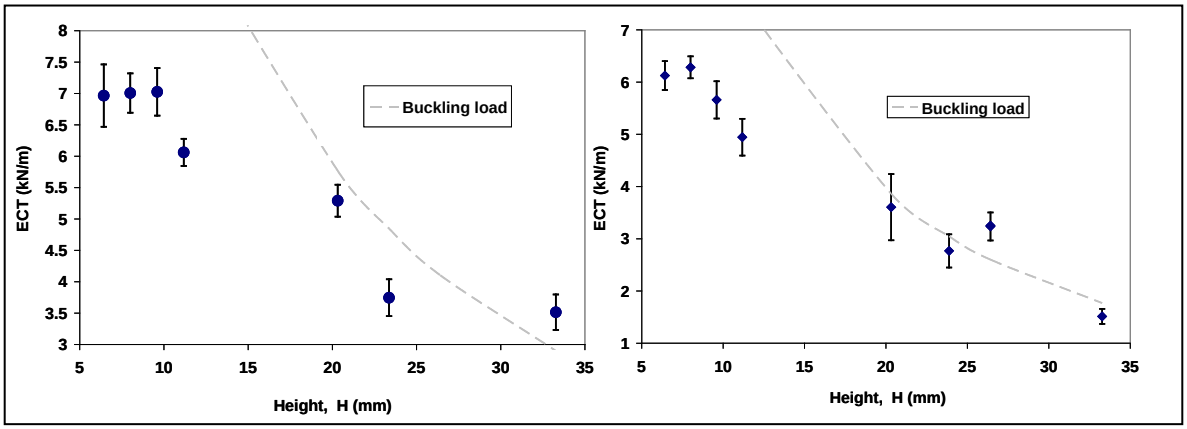

Figure 8. ECT versus free span height H using the T 839 clamping fixture for 42-23F (left) and 42-23N (right) board. Dashed curves represent calculated vertical buckling loads.

The plateau regions of constant ECT value appear to be overestimated by the buckling condition calculation, using (2) with the shear rigidity for E-flute as an approximation for F, N-flutes. Figure 6 indicates that the T 839 clamp method can be used for F-, N-flutes if the free span does not exceed 9 mm. This can be easily achieved by cutting these microflute samples to a height of 47 mm or smaller prior to their insertion into the T 839 clamping fixture.

The data presented here augment and substantiate the previous observations of the effect of specimen height on ECT (McKee 1961; Eriksson 1979; Kroeschell 1984; Wilson 2009). ECT values will decrease with increasing specimen height due to specimen buckling rather than specimen compression. Specimen heights for optimal ECT measurement fall approximately within the limits estimated by sandwich structure buckling. The implication here is that the beam mechanics shown here can be applied to other board configurations to estimate an appropriate specimen test height once measurements or calculations of the bending stiffness and measurements of shear rigidity are available.

COMPARISON OF TESTING METHODS ON CRUSHED BOARD

Much of corrugated board is crushed to some degree during manufacture either from the transfer press rolls or through die cutting scoring and slitting operations that are not optimally maintained. Although crushing is routinely assessed through a caliper

measurement, the strength losses in the medium are more evident in either bending stiffness (Eriksson 1979) or flat crush hardness or transverse shear (Popil *et al* 2006). A fluted medium weakened from crushing can produce an anomalously low ECT value similarly to the lightweight medium results shown in Fig. 1. More recently, Frank (2007) has shown that for many common commercially produced boards, enough transverse crushing occurs during the converting process such that the ECT clamping causes discrepancies between clamped and other common ECT methods. Therefore, it is of interest to determine whether the effects of crushing can be ameliorated by selection or modification of the ECT method.

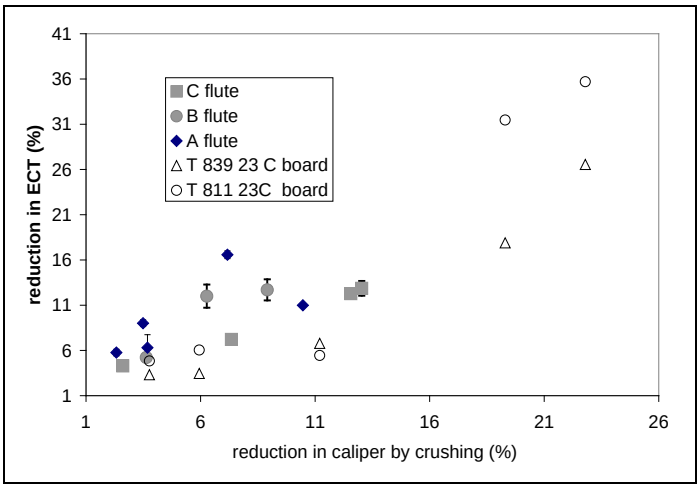

Figure 9. Summary of the loss of ECT of boards crushed to various levels

A series of boards were run through a motorized laboratory roller press nip running at 50 fpm with the roll gap separation set at various percentages of the original uncrushed caliper from 90 to 60 %. In these investigations, boards with fluting weight of 127 g/m^2 (26 msf) were of type A-, B-, and C-flute. Their final calipers after nip crushing were measured, and the ECT was evaluated using T 839. In addition, one series of C-flute boards with a lighter fluting weight of 112 g/m^2 (23 lb/msf) was also tested using both T 839 and T 811 methods, the results are summarized in Fig. 9 as the ECT loss as a function of caliper reduction. Generally, the crushing data indicates that ECT reduction is proportional to caliper reduction. The lightweight board 23-C data (open circles and triangles in Fig. 9) indicate that the waxed-end method results (triangular points) have lower ECT loss values than the clamp method results for low caliper reductions as expected, but the situation reverses at high crush values.

The difference between T 839 and T 811 ECT values for crushed boards is attributable to the effects of the clamping pressure on the board. Some measure of clamping pressure is required to secure the sample in place and prevent bending. (Schrampfer and Whitsitt 1988) examined the effects of clamping pressure on a series of corrugated boards and deduced for their sample sets of commercial boards that optimal correlation of T 839 results with T 811 occurs when the clamping pressure for T 839 clamp fixtures is in the range of 49 to 69 kPa. This was found to be an improvement from the original design pressure of 37 kPa. Accordingly, a prevalent commonly used design

from Emerson has springs with force constants stated to produce a typical clamping pressure of 69 kPa (Holmes 1996).

Applied pressure to the test specimen in T 839 comes from compressed springs extending behind the movable fixture jaws and so varies accordingly with the thickness of the inserted test board. Measurements of clamping pressure were taken using a small load cell (Interface Corporation) set in the open jaw gap, and the gap value was maintained by inserting shims of varied thickness. For example, an adequate pressure for thinner specimens such as miniflutes can be maintained by using shims placed behind the sample creating a jaw gap of a 3 or more mm. Linear interpolation of Table 2 data indicates the clamping pressure for E-flute board to be about 28 kPa for the Sumitomo fixture with no additional shimming.

Table 1. Measured Pressures for 2 Commonly Used ECT Clamps for Method T 839.

Jaw face gap	Sumitomo	pressure	Emerson	pressure
mm	kPa {lower}	kPa {upper}	kPa {lower}	kPa {upper}
3.18	39.7	41.3	33.0	30.5
4.47	49.9	46.2	42.9	35.2
5.72	59.2	53.3	54.4	50.6

Whether clamping effects can be eliminated through a change in technique was examined, since T 839 is a prevalent method and much of commercial corrugated board is crushed to some extent. The pressure of the clamps can introduce an initial convex profile of the board cross-section, leading to bending failure of the facings. Loss of ECT from crushing should only come from that portion of the medium that has become irreversibly creased or delaminated from the crushing action. The linerboard facings remain unaffected. An anomalous loss of ECT can arise from the bending failure arising from the initial convex bowing profile. Examination of magnified cross-sections of crushed board suggest that it is only the flanks of the fluting *i.e.*, a small percentage of the medium, about 10 to 15% of the total length of fluted medium, that is visibly irreversibly folded such that it can no longer contribute to compression strength.

Figure 10. Photograph of the dowel pin assemblies used to for crushed boards and T 839

Convex bowing of crushed board in the T 839 clamp was prevented by the use of dowel inserts into a single wall 42-26C commercial board. Dowel pin insert comb-like fixtures consisting of commonly available 3.2 mm diameter steel roll bearing pins, 19 mm long, were secured using epoxy resin ground to be flush with linerboard facings, as shown in Fig. 10.

These pin assemblies protruded 3 mm outside of the board edge when inserted. T 839 clamping pressures remain much the same for crushed boards as for uncrushed since boards recover over 90% of their original caliper (Koning 1986; Nordman *et al*. 1978; Kroeschell 1992) shortly after crushing. The jaw gap and accordingly, the applied pressure, will decrease somewhat for a crushed board.

Figure 11 shows the effects of crushing on ECT using the T 839 clamp with and without dowel pin inserts placed into the horizontal edges of the test specimens. The horizontal axis values are the gap setting of the crushing nip which ranges from 90 to 60% of the original caliper of the board. Results are compared using the neck-down method T 838, where failure is always observed at the neck of the specimen profile away from horizontal edges and there is no clamping of the test piece. The T 838 method results should be impervious to the artifacts induced by clamping pressure in T 839. A commercial circular cutting fixture (Lorentzen and Wettre) was used to prepare this width profile on square 50.8 mm specimens from the Billerud cutter.

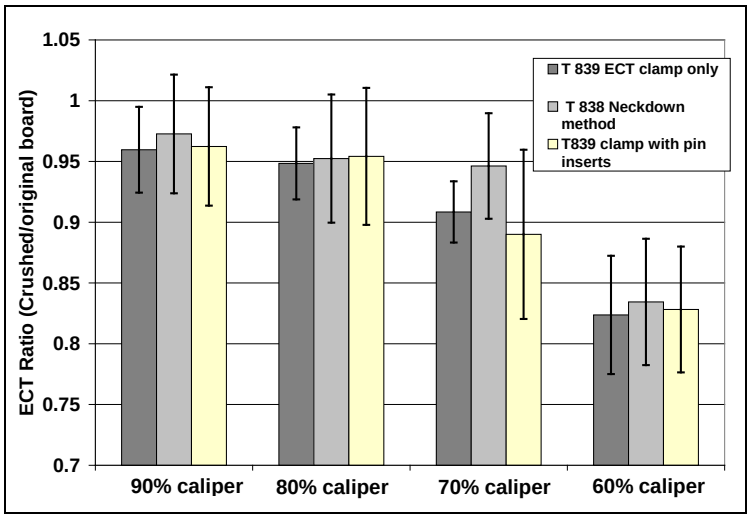

Figure 11. Ratio of measured ECT relative to uncrushed board using various methods. Horizontal axis indicates the level of crushing by a rolling nip gap expressed as a percentage of the original board caliper.

The 95% confidence interval error bars in Fig. 11 indicate that statistically there is no advantage of one method over the other in terms of the ECT being unaffected by the level of board crush. The results are essentially unaffected by change in testing method. At 60% crush level, we have ECT retention of 83% relative to the uncrushed board. The loss of 17% is consistent with the low power examination of crushed C-flute cross section and calculations of loss of contribution of the medium to ECT through the length-

weighted summation Equation (1). In this case for 127 g/m^2 C-flute crushed board, the use of dowel inserts in T 839 or T 838 did not demonstrate a difference from T 339, and the loss of ECT here is not considered anomalous. However, for other flute sizes or lightweight medium boards, the use of dowel inserts or T 838 may prove to be desirable to attain higher ECT values, as previously shown in Fig. 1.

EXPERIMENTAL OBSERVATIONS - EFFECT OF TEST DURATION

Since paper is a viscoelastic material, the rate of compression can be expected to have an effect on ECT. The test methods specify a compression platen advancement rate of 12.5 $\pm$ .25 mm/min. However, many European suppliers set the platen speed of their equipment at 10 mm/min, and other historically available data for ECT were obtained at differing strain rates. Quantification of the time relationship of ECT allows comparison of data sets obtained at differing strain rates. Therefore, experiments were conducted using resin-embedded and clamped C-flute samples placed in an Instron Universal tester such that the compression platen advancement rate varied from the default test value of 12.5 mm/min to 0.2 mm/min. ECT loads were recorded at the various platen rates along with time lapse video and load-displacement data to assess whether time duration has observable or measureable effects.

Figure 12 shows relationships of ECT platen rate dependence for resin-embedded and clamped specimens for a commercial 42-26C board. The effects of platen speed were found to be logarithmic (Moody and Koning 1996), in keeping with the generalization that strength properties drop about 7.5% per decade change in strain rate.

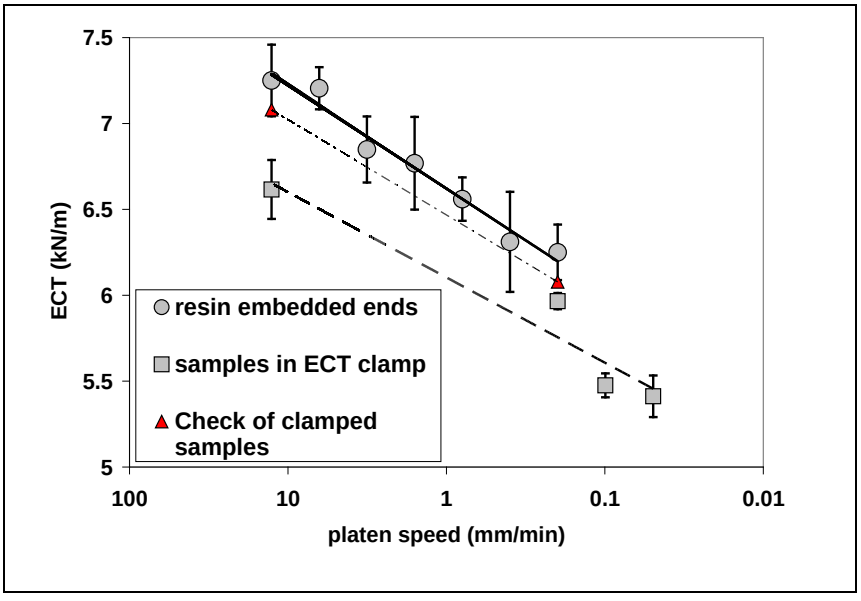

Figure 12. Observations of the ECT for C-flute sample at various platen strain rates using resin embedded samples (diamond points) and clamped specimens (squares and triangles)

Simple regression analysis reveals that the slopes and constants for the 3 sets of experiments shown in Fig. 10 are not statistically different, and the relationship can be summarized simply as,

$$ECT(kN/m) = 0.239 \times \ln(v) + 6.47 \ \pm \ 0.01 \quad (4)$$

where v is the platen speed in mm/min and the mean error of the regression fit in (4) follows the $\pm$ sign. Normalizing the data with respect to the ECT measured at the TAPPI prescribed speed of 12.5 mm/min designated as $ECT_{(Tappi)}$, the time series data can also be summarized in the convenient form:

$$\frac{ECT}{ECT_{(Tappi)}}\ (\%) = 3.11 \times \ln(v) + 91.7 \ \pm \ 0.4 \quad (5)$$

Equation (5) indicates a 6.2% drop in ECT to occur for every decade of change in rate of strain. The implication of this result (5) can be considered in the storage of vertically loaded boxes. In many cases, the requirement for vertically loaded boxes is to sustain a load for about a month. Examination of individual test load-displacement data generally show that specimens fail in the compression test usually at around 1.6 % strain. This was consistently observed to be invariant of the platen speed v in the course of the experiments for C-flute time series. Therefore, for a month-long stacking requirement, the strain rate to failure is 1.88 x 10^{-6} mm/min. Substitution of this rate for v into (5) finds that the ECT is reduced from its TAPPI test value by 51%. For boxes whose longevity in stacking is primarily determined by their ECT, this result suggests that the safety factor for a duration of one month the safety factor (failure load/applied load) for ECT should be 2.

INTERFLUTE BUCKLING AFFECTING ECT

A patterned dimpling of linerboard facings is often commonly observed in corrugated fiberboard containers that have been placed under a vertical stacking load and exposed to a high humidity environment (see Fig. 13).

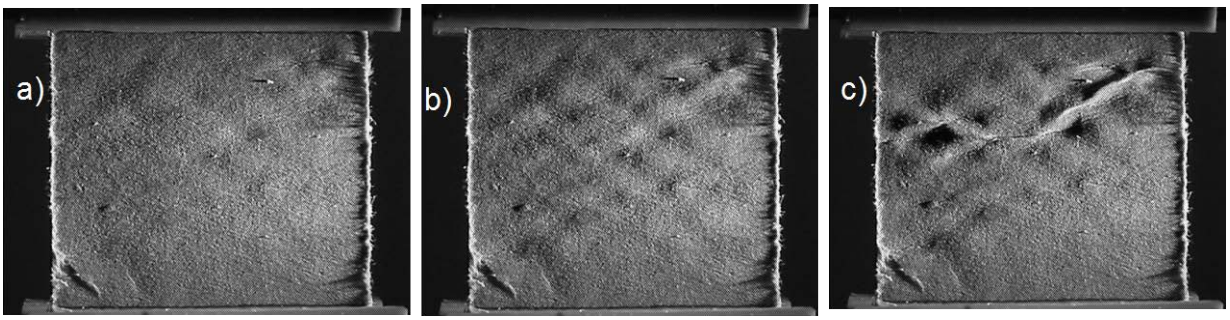

Figure 13. Excerpted time sequence video snapshots of a glancing angle illuminated ECT test of a 35-26C flute board: a), 5.7 kN/m load, 1.3% strain, some buckling is evident b), peak load 6.7 kN/m, 1.6% c), post failure 4.5 kN/m, 2.1% , crease forms joining micro-plate buckling crests

The same dimpling or localized buckling is also observed to occur during the ECT of large-flute (A or C) lightweight corrugated boards. A series of time resolved video recordings of the ECT various boards were made with the frames synchronized with load-displacement data. An example of a few selected frames from one such series is shown in Fig. 13, which tested a 35-26C board mounted in supporting resin platforms.

Glancing angle collimated illumination from the right has side in Fig. 11 was used to highlight features on the linerboard. Visible dimpling of the facing is observed to progressively form as the load increases near to the peak value. Once peak load is reached, a crease immediately forms, and it progressively develops, joining the crests of the buckled areas across the width of the sample. For boards with small flute size (B or E) or heavyweight linerboard facings, no buckling patterns are observed, only the formation of a crease at peak load appears. This was confirmed by video observation of a variety of laboratory prepared boards as reported by Schaepe 2006.

Urbanik (1990) of the Forest Products Laboratory (FPL) noted localized buckling behavior in the vertical loading of corrugated board and accordingly applied a non-linear theory to describe the ECT failure load in terms of plate mechanics. The corrugated board is considered as consisting of a series of infinitely long plates with the ends at the glue lines being free to rotate, the so-called simply-held end condition. The board is considered to fail either through buckling or through a combination of compression and buckling. Component response behavior is modeled through non-linear fit of the load deformation compression data of the facing and medium obtained from a specialized restraining apparatus that excludes buckling during testing. Predictions for the ECT value for a board are numerically computed based on these premises. This FPL model follows an earlier non-linear buckling model presented by Koning (1975, 1978), which calculates the ECT of the board as the buckling load of a panel. Dimitrov (2009) points out that these models require load deformation data using specialized restraining equipment and sophisticated computer analyses.

Bormett (1986) provides a lucid comparison of the FPL model and simpler analytical models for ECT. The maximum load equal deformation model presented by Equation (1) excludes any localized or other bending of the board and neglects that the medium is expected to fail sooner than the linerboards as the strain in the test increases. Hence, for this and other considerations, the constant in front of the length weighted summation of the component compression strengths in Equation (1), is around 0.7

A Model for ECT with Component SCT and Bending Stiffness

The motivation for this model is to provide a simple means for accounting for localized interflute buckling while using commonly available testing data. An improved accuracy in predicting ECT should result. The effects of increased compression strength with accompanying decrease in bending stiffness that occurs with high pressure wet pressing can be quantified. The model is similar to the FPL work in that the facings are considered to consist of infinitely long plates simply supported on their unloaded edges by the glue lines. The micro-plates can buckle with an applied vertical load. The facings can buckle provided that their bending stiffness is sufficiently small such that a compression failure crease does not occur as the stress increases in an ECT. The facings fail either through combined buckling and compression, dubbed postbuckling behavior,

as observed in Fig. 11, or simply just by compression creasing without buckling according to observations of ECT.

The medium can buckle in ECT as well under the right circumstances as shown by Urbanik (1990). However, for simplicity, the buckling of the medium is not considered in the model, although incorporation of its buckling is a straightforward extension of the considerations applied to the linerboard micro-plates. The basis weight of the medium considered here is 127 g/m^2 (26 lb/msf), and it is assumed not to buckle during ECT but fail only by compression creasing. The curvature of the fluting imparts an additional structural rigidity to the medium.

A key result from plate mechanics for an orthotropic plate of constant thickness used in the model is the critical buckling load for an infinitely long plate of width b_f.

$$P_{cr} = \frac{4\pi^2\sqrt{D_{11}D_{22}}}{Kb_f^{\ 2}} \quad (6)$$

In this equation $\sqrt{D_{11}D_{22}}$ represents the geometric mean (MD-CD) flexural rigidity of the plate, b_f is the flute spacing, and K is a constant ≤ 1, depending on the restraint to rotation offered at the flute tips, for simply supported plates K =1. For simplicity and to a good approximation, Poisson terms are neglected and flexural rigidity and bending stiffness are considered to be equal. Note that the buckling load for plate Equation (6) is similar but is different than the previously considered expression for the buckling of a beam P_E. Calculations for the buckling load of fluted medium can be made using the expressions for the flute geometry specified by Urbanik (2001) along with the stress to vertically buckle a thin-walled tube (Shallhorn 2005). For example, a C-flute 127 g/m^2 medium micro-plate will have an effective b_f of 1.7 mm, much reduced from glue line spacing of 7.8 mm, MD and CD bending stiffnesses 5.3 and 2.9 mN-m respectively, which lead to a P_{cr} of 53.4 kN/m, which is much higher than typical C-flute ECT values. Moreover, the crests of the C fluting have a radius of 1.7 mm, a medium CD modulus of 1.6 GPa, and a caliper of 249 microns, which lead to calculated tube buckling loads of 1510 kN/m.

Video recordings were made of A-flute 127 g/m^2 adhered to clear plastic film and subjected to vertical load. In this case, calculations indicate that the buckling load for the flat portion of the fluting is 12.6 kN/m and for the curved portion of radius of 1.5 mm, the calculated buckling load is 209 kN/m. Both calculated buckling load values are quite far from typical C- and A-flute ECT values. The video record of A-fluting adhered to plastic film showed no buckling prior to a compression crease failure coinciding with plastic film creasing.

Numerical simulation of ECT using the material constants for the laboratory-made boards used in this study were made using a non-linear constitutive model with geometric nonlinear effects (Haj-Ali *et al*. 2008). The patterned out-of-plane dimpling occurs in the simulations corresponding to experimental video observations. The magnitude of the out-of-plane displacement of the buckling pattern of the 205 g/m^2 linerboard facings is as much as 0.3 mm in the simulations. The computations indicate no corresponding buckling for the 127 g/m^2 medium.

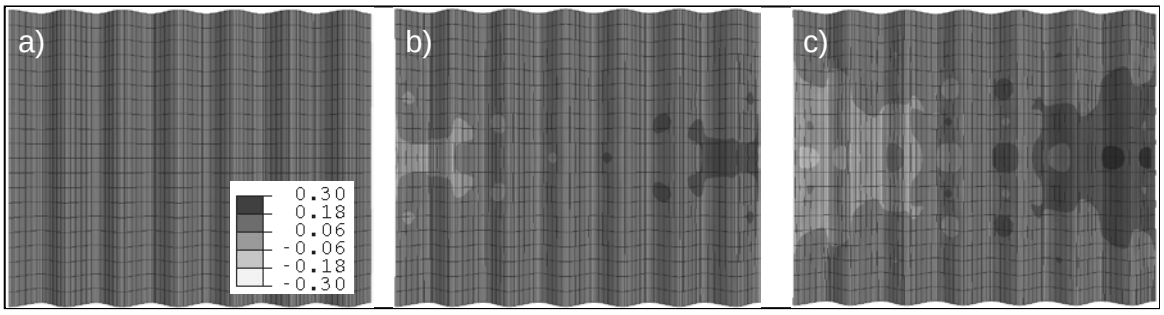

Figure 14. Progressive out-of-plane displacement maps for the C-flute medium from a nonlinear FEA ECT simulation from Haj-Ali *et al*. (2008)

Figure 14 shows the progressive calculated out-of-plane displacements for the medium for C-flute simulation data presented in detail in Fig. 10 of Haj-Ali *et al*. (2008). At point a), the failure initiates with the facing (not shown in Fig. 14 here), starting to show a patterned buckling and a Tsai-Wu failure criterion (shown in Haj-Ali Fig. 10) is met locally corresponding to the start of a formation of a crease, where the medium (shown in Fig. 14 above) shows no patterned buckling. Point b) is at the ultimate failure stress level as determined by the Tsai-Wu criterion linking several failed regions across the width of the board. There is a prevalent predicted out-of-plane buckling for the facings resembling b and c of Fig. 13. However, the medium in Fig. 14 shows negligible buckling. Results are also shown for a third calculation c), for the case of the vertical displacement being 2X from the failure initiation point. Here, the failed regions, as indicated by contours on the facings satisfying the failure criterion, become fully linked across the width of the board, corresponding to a crease.

Hence, video observations, analytical, and numerical simulations all indicate that the 127 g/m^2 medium will not buckle in ECT, but the linerboard facings will buckle between the flute lines, provided that their compression strength exceeds their buckling load. If the linerboard facings buckle, it is expected that their ultimate strength will be governed by the empirical expression for plate failure load P_z,

$$P_z = cP_m^b P_{cr}^{1-b} \tag{7}$$

where, per unit length, P_m is the intrinsic compression strength of the material, P_{cr} is the critical buckling load given by (6), and c and b are empirical constants. Equation (7) is the basis for the derivation for the McKee equation for the compression strength of boxes consisting of linked buckling panels with P_m as *ECT* of the corrugated board. By similar reasoning, *ECT* consists of buckling linerboard plates whose P_m is now taken as the short span compression strength *(SCT)*. Thus, for a single wall board, the model for *ECT* considered as the equivalent of P_z is written as:

$$\begin{aligned} ECT &= C'\left\{2\times (SCT)_l^{\,b}(P_{cr})^{(1-b)} + \alpha(SCT_m)\right\} \ \textit{if} \ \ (SCT)_l \geq P_{cr}, \ \textit{buckling occurs} \\ &= C\left\{2\times (SCT)_l \ + \alpha\,(SCT)_m\right\} \textit{ if } \ P_{cr} \ \geq (SCT)_l, \ \textit{equation (1) applies} \end{aligned} \tag{8}$$

Application of (8) to multiwall boards is straightforward with the addition of similar terms to account for additional board components and different medium take-up factors.

Experimental Verification of the ECT Buckling Model

Verification of the model was made by preparing a series of linerboards in various ways, measuring their ECT using T 839, and comparing the data with predicted values using a fitted model. In all data sets, presented in Table 2, the relevant physical properties of the components were measured: caliper, basis weight, CD SCT, and MD and CD Taber stiffnesses. The bending stiffnesses and flute spacing was used to calculate P_{cr} using (6) and K=1. It should be noted that the calculation of P_{cr} using bending resistance values from the popular Taber instrument require multiplication of the results by 1.67, since these values represent bending moment and not stiffness (Carson and Popil 2008). The bending stiffness values reported in the relevant previous work of Whitsitt (1988) are too low because this issue was overlooked. If the calculated P_{cr} was less than linerboard *SCT*, thus indicating the likelihood of facing buckling during vertical compression, constants C' , b and K were fitted by regression analysis to the ECT data, otherwise only the constant C in Equation (1) was fitted.

One series of boards produced on a pilot single facer contained embedded spliced handsheet linerboards of various basis weights pressed to various densities. This is similar to the investigation previously reported by Whitsitt (1988), where linerboard handsheets of various basis weights were pressed to different densities to obtain a range of increasing compression strengths. The furnish composition of the linerboard and medium were constant throughout the series of prepared handsheets. The prepared linerboard handsheets were individually manually spliced into conventional linerboard rolls that were run through the pilot single-facer corrugator at IPST using conventional corrugating operating parameters. Double-backing of the prepared single face samples was performed manually on long sheets of single-facing using a metered roller to apply Stein-Hall starch adhesive and a hot plate press to produce single-wall corrugated board samples consisting of, in this case, variable density handsheets adhered to 127 g/m^2 C-flute medium.

A second series of boards were prepared using commercial linerboard and medium with various flute sizes and combinations using the IPST pilot plant facilities as described in detail by Schaepe and Popil (2005). In the second series, the linerboard and medium were the same throughout and had the properties for the C-flute board data shown in Table A1. The ratio of buckling load P_{cr} to $(SCT)_l$ shown in the last column in Table 2 shows that many of the boards investigated in this program can be expected to display interflute buckling whenever the ratio is less than one. For the case of multi-wall board samples, a single $P_{cr}/(SCT)_l$ ratio value is reported in the Table column only for the liner facing expected to buckle.

A third series of boards selected for ECT buckling investigations consisted of commercial linerboards and medium supplied directly from the corrugator as unconverted cut sheets. The linerboard and medium for these boards were separately provided for physical property measurements.

The analysis is divided into the classes of boards. In each case, a multi-parameter fit for the constants *C*, *C'*, *K*, and *b* was applied to the sets of data using the model represented by Equation (8). Fitting was done by iteratively reducing the error between the model and actual data using numerical routines such as the Solver algorithm in MS Excel.

Table 2. Summary of Corrugated Boards and Selected Properties Used in the Investigation of Interflute Buckling

Combined Board Sample ID	Sample description	Medium flute size	caliper of combined board (microns)	basis weight of combined board (gms)	CD SCT liner (kN/m)	liner density g/cm^3	CD SCT medium (kN/m)	liner Taber moment geometric mean (g-cm)	T 839 ECT kN/m	Buckling load/SCT
WC 35-26C-35	commerical lighweight C flute board	C	4140	542	3.9	0.82	2.1	25.4	7.6	0.72
WC 35-26C-35 ipst	IPST lab board same components as above	C	4100	583	3.9	0.62	2.1	25.4	8.4	0.72
WC 35-26E-35	commerical E flute board	E	1620	521	3.9	0.69	2.1	25.4	8.1	3.68
WC 42-26C-42	Standard commerical C flute board	C	4210	605	3.4	0.68	2.1	31.4	7.9	1.02
WC 42-26C-42 ipst	IPST lab board same components as above	C	4130	646	3.4	0.69	2.1	31.4	8.7	1.02
WC 56-26C-56	commerical heavyweight board	C	4350	748	5.3	0.84	2.1	65.7	11.2	1.34
WC 56-26C-56 ipst	IPST lab board same components as above	C	4290	757	5.3	0.70	2.1	65.7	10.9	1.30
GP 26-23C-26	commerical lightweight C fluteboard	C	3838	420	2.4	0.68	2.1	8.5	5.3	0.38
GP 35-26C-35	commerical light standard C fluteboard	C	3967	507	3.7	0.66	1.9	19.1	6.8	0.56
GP 42-33C-42	commerical standard C fluteboard	C	4046	575	3.9	0.59	2.2	31.1	7.9	0.87
GP 55-33C-55	commerical heavyweight C fluteboard	C	4334	783	5.3	0.60	2.2	62.6	11.0	1.28
TI 42-23E-42	commerical E flute board	E	1691	581	3.8	0.72	1.7	27.0	8.0	3.99
TI 35-23C-35	commerical lighweight C flute board	C	4067	547	3.7	0.70	2.4	20.2	7.8	0.60
TI 56-23C-56	commerical heavyweight C flute board	C	4207	751	5.4	0.70	1.8	63.8	10.8	1.29
IPST 42-26C-35	IPST lab asymmetric board	C	4214	580	4.6	0.70	2.4	42.2	8.6	0.96
IPST 42-26C-55	IPST lab asymmetricboard	C	4443	687	4.6	0.70	2.4	42.2	10.6	0.96
IPST 42-26E-42-26C-42	IPST lab multi-wallboard	C & E	5679	1019	4.6	0.70	2.4	42.2	16.3	0.96
IPST 42-26A-42	IPST lab A flute board	A	5171	624	4.6	0.70	2.4	42.2	8.5	0.81
IPST 42-26B-42	IPST lab B flute board	B	3044	599	4.6	0.70	2.4	42.2	9.9	1.64
IPST 42-26A-42-26B-42	IPST lab multi-wall board	A & B	7933	1014	4.6	0.70	2.4	42.2	14.9	0.81
IPST 42-26A-42-26C-42	IPST lab multi-wallboard	A & C	9015	1011	4.6	0.70	2.4	42.2	14.9	0.81
IPST 42-26B-42-26C-42	IPST multi-wall lab board	B & C	6959	1026	4.6	0.70	2.4	42.2	15.3	1.64
IPST 42-26C-42	IPST lab C flute board	C	4252	613	4.6	0.71	2.4	42.2	9.8	0.96
IPST 42-26C-42	IPST lab C flute board	C	4215	588	4.6	0.69	2.4	42.2	9.6	0.96
IPST 42-26E-42 trial run	IPST lab E flute board	E	1660	582	4.1	0.70	2.3	33.4	7.9	4.58
IPST 42-26E-42	IPST lab E flute board	E	1642	591	4.6	0.70	2.4	42.2	10.6	5.16
N&W 100 low press	IPST lab 100 gsm handsheet board	C	4063	421	1.8	0.40	2.4	20.4	4.7	1.18
N&W 100 med press	IPST lab 100 gsm handsheet board	C	3958	420	2.1	0.52	2.4	11.4	4.5	0.56
N&W 100 high press	IPST lab 100 gsm handsheet board	C	3956	427	2.6	0.62	2.4	2.1	4.7	0.09
N&W 200 low press	IPST lab 200 gsm handsheet board	C	4352	634	3.6	0.41	2.4	78.2	7.6	2.27
N&W 200 med press	IPST lab 200 gsm handsheet board	C	4109	640	5.1	0.58	2.4	43.0	8.6	0.87
N&W 200 high press	IPST lab 200 gsm handsheet board	C	4092	629	5.9	0.71	2.4	32.3	8.4	0.57
N&W 300 low press	IPST lab 300 gsm handsheet board	C	4700	845	4.5	0.41	2.4	228.6	9.2	5.32
N&W 300 med press	IPST lab 300 gsm handsheet board	C	4357	871	6.6	0.56	2.4	161.8	10.5	2.54
N&W 300 high press	IPST lab 300 gsm handsheet board	C	4324	895	7.7	0.64	2.4	152.3	11.1	2.06
N&W 100-100 psig	IPST lab 100 gsm handsheet board	C	4357	390	1.5	0.44	2.4	8.9	4.5	0.61
N&W 100-400 psig	IPST lab 100 gsm handsheet board	C	4324	390	2.0	0.61	2.4	4.9	4.4	0.26
N&W 100-1900 psig	IPST lab 100 gsm handsheet board	C	4507	390	2.2	0.80	2.4	2.3	4.5	0.11
N&W 160-100 psig	IPST lab 160 gsm handsheet board	C	4179	527	2.8	0.48	2.4	35.9	6.1	1.35
N&W 160-400 psig	IPST lab 160 gsm handsheet board	C	4147	530	3.5	0.64	2.4	27.0	6.2	0.79
N&W 160-1900 psig	IPST lab 160 gsm handsheet board	C	4025	535	4.0	0.85	2.4	13.3	7.0	0.34
Formette Sheet 100- 0 psi	IPST lab oriented 100 gsm handsheet board	C	4105	410	1.1	0.29	2.4	17.4	3.9	1.69
Formette Sheet 100-50 psi	IPST lab oriented 100 gsm handsheet board	C	4068	412	1.5	0.51	2.4	6.2	4.3	0.44
Formette Sheet 200-0 psi	IPST lab oriented 200 gsm handsheet board	C	4263	638	2.2	0.30	2.4	104.0	6.5	4.82
Formette Sheet 200-50 psi	IPST lab oriented 200 gsm handsheet board	C	4145	645	3.8	0.58	2.4	49.7	6.9	1.38

Figure 15 shows the comparison of predicted ECT values from the model to actual ECT values for the series of laboratory made boards using spliced handsheets. In cases where buckling of the facings occurs, the model places the predicted adjusted values closer to the identity line, reducing the error. Constants *C'*, *C*, *b*, and *K* were determined to be 0.72, 0.7, 0.65, and 0.96, respectively. The fact that the value of *K* was close to one supports the model of linerboard plates between glue lines being simply supported at the unloaded vertical edges at the glue lines. The regression R^2 value

increases from 0.91 to 0.94 when the buckling model (8) is used instead of (1), and the mean error correspondingly is reduced from 0.19 to 0.16 kN/m.

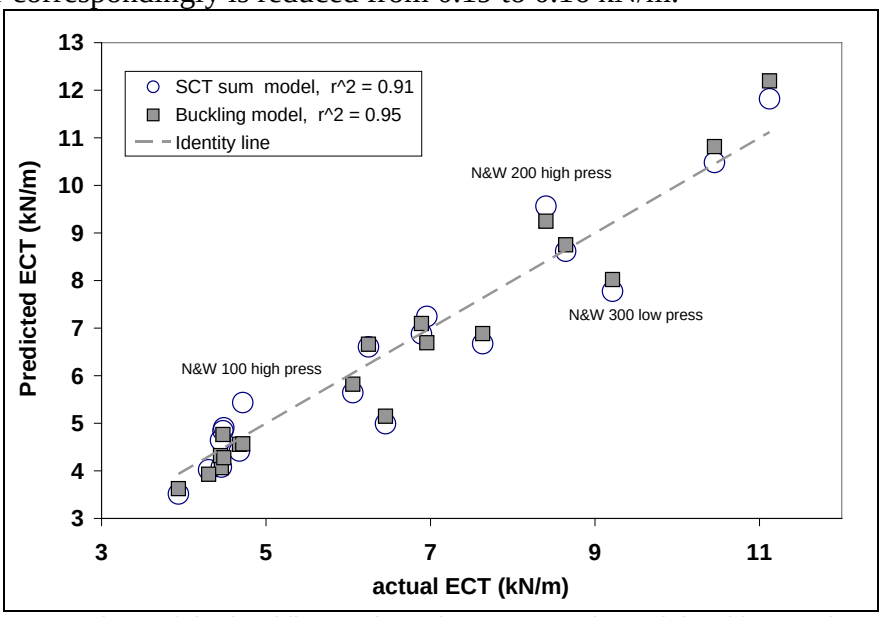

Figure 15. Comparison of the buckling and maximum strength models with actual ECT for laboratory made corrugated boards using spliced handsheets

The controlled wet pressing of handsheets allowed a large range of densities of handsheets to be prepared such that relationships between the *SCT*, $\sqrt{D_1 D_2}$, and basis weight could be determined, as shown in Fig. 16.

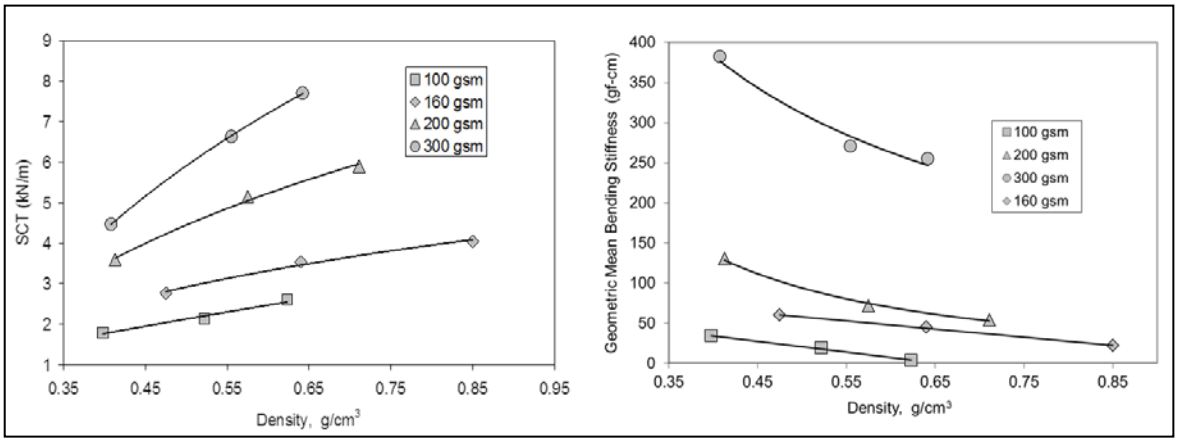

Figure 16. Relationships between and geometric mean bending stiffness versus density for the handsheets used in the corrugated board test results shown in Fig. 15

As shown by Whitsitt (1988), increasing the compression strength *SCT* through wet pressing decreases the bending stiffness and ultimately places a limit on the *ECT* that may be gained through wet pressing. With increased wet pressing, the density increases, and *SCT* increases as well as a result of more fiber bonding as may be expected from first principles (Shallhorn *et al*. 2004). However, the bending stiffness simultaneously

decreases as a result of reduced caliper. Therefore, the increase in *SCT* from a wet pressing density increase is compromised by a corresponding decrease in bending stiffness, and this phenomenon is accounted for in the buckling model (8) for ECT. The respective values for SCT and $\sqrt{D_1 D_2}$ for each basis weight sample set was substituted into the ECT buckling model with fitted constants to produce a series of predicted ECT values for each basis weight class as a function of the wet pressed density. Figure 17 summarizes these calculations, which show optimal densities are reached for maximum *ECT* in lightweight linerboards adhered to 126 g/m^2 C-flute medium.

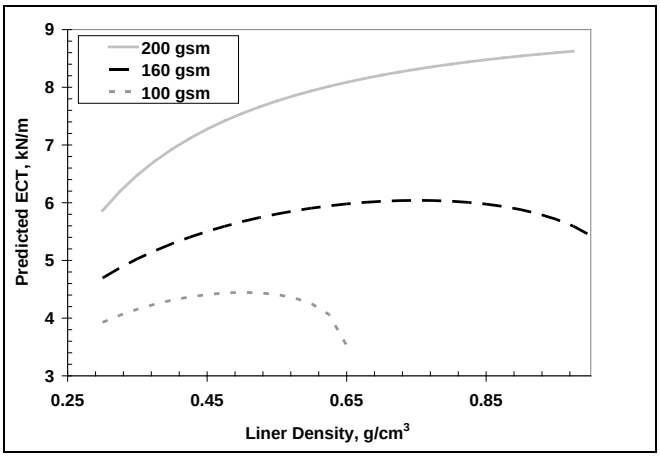

Figure 17. Summary of calculations for predicted ECT using buckling model (8) and fitted constants derived from the handsheet data set of Fig. 13

The set of laboratory-made boards was augmented by another series using different flute sizes and are denoted by the prefix "IPST" in Table 2. The linerboard and medium components were the same throughout this series of boards. Video observation of the ECT of these boards confirmed the prediction of Equation (6) with *K* set to 1 for buckling onset. Namely, for the linerboard properties used in this series, Equation (6) predicts that A- and C-flute boards will buckle when placed under vertical load, but B- and E-flute boards will not. The smaller flute size b_f for B- and E-flute board makes the ratio $P_{cr}/SCT > 1$ for the selected materials' properties, and so no buckling is expected. Video recordings of the ECT testing of multi-wall boards of both single-face and double-back sides simultaneously (Schaepe and Popil 2006) showed the separate development of interflute buckling or compression failure depending on the particular flute size adhered to the specific facing. The summary of results for this set, including the embedded handsheet board sheet, is shown in Fig. 18 where again, the overall correlation improves from $R^2 = 0.91$ to $R^2 = 0.94$ when buckling is considered, and the mean error between predictive model and actual values becomes smaller, from 0.16 to 0.14 kN/m.

A confirmation of the application of the model was applied to a series of commercial boards obtained from box plants. These boards were all C-flute, with different basis weight liners and medium. The results shown in Fig. 19 indicate, as expected, that the largest differences occur when the model is applied to lightweight boards 23-23C and 35-26C, which in this data set have the effect of improving the

correlation of predicted with actual values from R^2 =0.90 to R^2 =0.97 and reduced error from 0.18 to 0.09 kN/m.

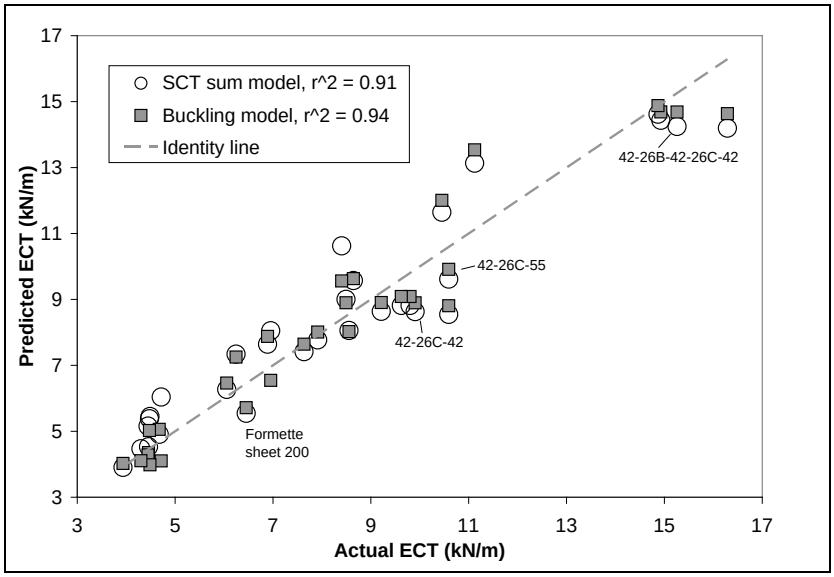

Figure 18. Summary comparison of all lab-made corrugated board predicted and actual ECT values

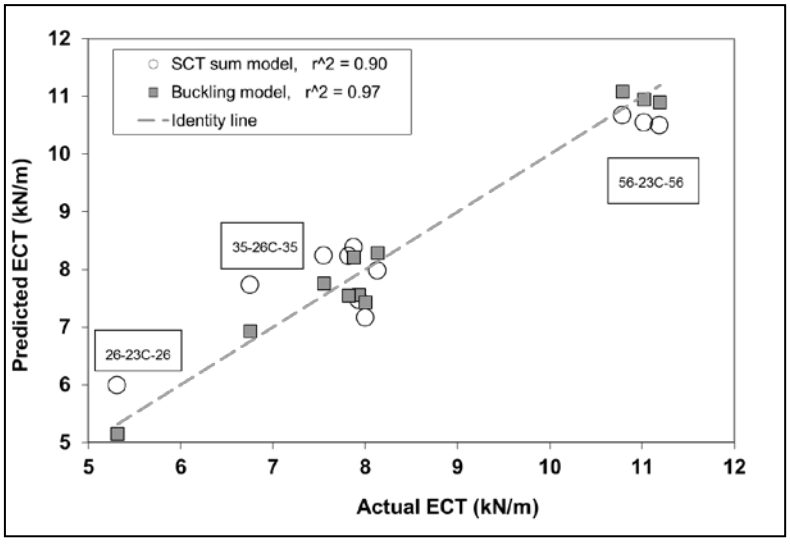

Figure 19. Predicted and actual ECT values for a series of commercially produced C-flute boards

Use of Equation (8) to predict ECT to supplant Equation (1) accounts for the effect of interflute buckling of the facings in lightweight boards and reduces the error in predicting ECT. The model predicts an optimal density from wet pressing that limits the gains obtained in linerboard compression strength. The postbuckling predictive model (8) uses measurements that are commonly available in most paper testing laboratories and is

straightforward to implement through simple calculation. The summary of the constants for the various sample sets are summarized in Table 3.

Table 3. Summary of Model Fits for Several Corrugated Board Data Sets. *

Data Set	ECT Model	C or C'	b	K	r^2	MSE
1. all IPST lab made board	SCT sum	0.70			0.91	0.19
	Buckling	0.72	0.65	0.96	0.94	0.16
2. Commercial boards	SCT sum	0.77			0.90	0.18
	Buckling	0.80	0.71	1.16	0.97	0.09
3. IPST spliced handsheet boards	SCT sum	0.70			0.91	0.16
	Buckling	0.65	0.85	1.18	0.95	0.14

* MSE is the mean square-root error for each fitted model.

CONCLUSIONS

The edge compression test of combined corrugated board was considered in this paper to provide guidance for the interpretation and qualification of testing results. Investigations into the testing techniques arose as a result of an IPST research program on corrugated container performance. Different measurement techniques were examined for their applicability. In particular, various aspects of the T 839 clamp method were investigated: the effect of span, duration of the test, and effects of clamping on crushed board. Calculations and experiments were applied to a selected common set of C-, E-, F- and N-flute samples. Beam mechanics applied to the data support the concept that corrugated C-, E-, F-, and N-flute boards in a T 839 clamp behave as simply held sandwich structures and display a predictable fall in measured compression strength with increasing test specimen height. The T 839 clamp method, as is, can be used for 42-26C boards to obtain a reliable measurement. Method specifications of specimen height appear to be conservative. The micro-flutes 42-23E and 42-23F can also be tested in T 839 if the test samples are cut 5 mm shorter (45 mm height) prior to placement in the clamp. When testing thin boards such as micro-flutes, the jaw gap should be maintained at a few mm to maintain clamping pressure by the use of shims placed in the jaws against the test samples.

A study of ECT involving 42-26C boards crushed out-of-plane to varying degrees used several different methods to determine whether effects of clamping pressure can be mitigated. Neither use of T 838 neck down method nor the inclusion of dowel inserts maintained the ECT value of the board before crushing. Out-of-plane crushing to 60% of the original caliper causes an estimated 16% loss in compression strength of the fluted medium.

A study of platen rate effect on ECT confirms that ECT will decrease with the logarithm of the rate, in agreement with previous reports. Discrepancies of about 1-2% can be attributed to differences in common compression tester platen speeds. The strain rate dependence results are presented in a form convenient for application of correction factors to compare intra-laboratory results.

Investigations of the fluting of facings between glue lines in ECT of lightweight boards led to a conveniently applied model based on postbuckling behavior of plates. Fits of the data indicate that the buckling onset load can be predicted by a simple expression from plate mechanics for vertically loaded plates with simply supported edges. Standard laboratory measurement of the linerboard and medium SCT along with the linerboard bending stiffness can be used to obtain an improved calculated prediction of the expected ECT value. The results show for lightweight boards how increased wet pressing will increase the severity of interflute buckling and thus limit ECT.

ACKNOWLEDGEMENTS

Funding support was provided by the IPST Industry Member companies participating in the IPST Engineered Packaging Consortium program starting in 2002. Former IPST professors Doug Coffin and Chuck Habeger were principally involved as initiators of the project. A portion of the data presented on inter-flute buckling is part of the IPST MSc thesis of Pacharawalai Kaewmanee. Leif Carlsson kindly supplied an English version of his cited 1985 paper on the calculation of corrugated board bending stiffness used in Table A1.

APPENDIX A:

Validity of the Sandwich Beam Approximation for Corrugated Board

The validity of approximating corrugated board as a sandwich structure used to justify (3) is examined by a comparison of calculations and measurements for the bending stiffness. Samples of corrugated board and their individual corresponding components were obtained from commercial manufacturers and their physical properties measured using standard TAPPI methods (Carson and Popil 2008). Physical properties for a selected series of C-, E-, F-, and N-flute boards and their components are listed in Table 1. The elastic moduli for linerboard E_l and medium E_m were obtained from analyses of tensile test data. Bending stiffness measurements D_{CD}*(meas.)* were made using the 4 point bending method T 820, which excludes out-of-plane shear by its testing configuration. In Table A1, the medium to linerboard length ratio, called the take-up factor is α, linerboard, medium, and board thicknesses are t_l, t_m, and h respectively.

Table A1. Summary of Relevant Properties for Single-wall Corrugated Boards*****

Flute type	α	E_l	E_m	t_l	t_m	h	D_{CD} *(meas.)*	$D_{CD\ sand}$	*Ranger*	Nordstrand	Carlsson	R_{44}
		GPa	GPa	mm	mm	mm	N-m	N-m	N-m	N-m	N-m	kN/m
C	1.42	2.09	1.61	0.29	0.25	4.21	5.2	5.37	5.28	5.31	5.45	54.3
E	1.27	1.72	1.13	0.24	0.19	1.64	0.7	0.56	0.44	0.44	0.6	20
F	1.25	1.74	1.14	0.29	0.22	1.37	0.41	0.47	0.31	0.32		
N	1.2	1.74	1.14	0.29	0.22	1.07	0.23	0.29	0.16	0.16		

* Measured Bending Stiffness is D_{CD} *(meas.).* Calculated Estimates for Bending Stiffness are: $D_{CD\ sand}$, Ranger, Nordstrand and Carlsson. Measured Shear Rigidity in the CD is R_{44}.

A simple approximation often used for bending stiffness of corrugated board is,

$$D_{CD\,sand} \approx \frac{E_l t_l h^2}{2} \quad \text{(A1)}$$

which neglects the contribution of the medium to bending stiffness of the combined board. Nordstrand (1995) compares approximating the corrugated board as sandwich structure with a more exact calculation (Carlsson *et al*. 1985) and finds the agreement to be within 4%. In this case, the corrugated core of the sandwich structure is homogenized as an equivalent layer in a laminate structure (*e.g.*, Bodig and Jayne 1982) having an effective modulus equal to $\alpha E_m t_m/(h - 2t_l)$, since $h\text{-}2t_l$ is the thickness of the fluted core. The full expression for the bending stiffness for the sandwich structure including the contribution of the medium becomes:

$$D_{CD} = \frac{1}{2} E_l t_l \left(h^2 - 2ht_l + t_l^2\right) + \left\{\alpha \frac{E_m t_m}{12}\left(h - 2t_l\right)^2\right\} \quad \text{(A2)}$$

The expression (A2) corrects a typographic error in Nordstrand (1995). Schick and Chari (1965) also cite an earlier formulation by Ranger in which the corrugated medium contribution term (contained in curly brackets in (4)) is calculated by integration to be $(1/2\pi)E_m t_m(h - 2t_l - t_m)^2$.Table A1 shows that the sandwich beam approximations (A1) and (A2) as well as more exact calculations by Carlsson and Ranger all agree well with the measured bending stiffness for the selected board set.

REFERENCES CITED

Allan, R. J. (2007). "Development of a new measurement for board performance," *61st Appita Annual Conference and Exhibition, Proceedings,* Vol. 1, Gold Coast, Australia 6-9 May 2007, Appita Conference Papers, 151-158.

Batelka, J. J. (1994). "The effect of boxplant operations on corrugated board edge crush test," *Tappi Journal* 77(4), 193-198.

Bodig, J., and Jayne, B.A. (1982). *Mechanics of Wood and Wood Composites,* Van Norstrand Reinhold Company, New York.

Bormett, D. W. (1986). "Predicting edgewise compressive strength," *Boxboard Containers* 94(4), 30-34.

Carlsson, L., Fellers, C., and Jonsson, P. (1985). "Bending stiffness of corrugated board with special reference to symmetrical and multi-wall constructions," *Das Papier* 39(4), 149-157 (in German).

Carson, C. G., and Popil, R. E. (2008). "Examining interrelationships between caliper, bending and tensile stiffness of paper in testing evaluation," *Tappi Journal* 7(12), 17-24.

Dimitrov, K., and Heydenrych, M. (2009). "Relationship between the edgewise compression strength of corrugated board and the compression strength of liner and fluting medium papers," *Southern Forests* 71(3), 227-233.

Eriksson, L. E. (1979). "A review of the edge crush test boxboard," *Containers International* 86(8), 34-38; 86(9), 64-67.

Fiber Box Association (2009). *Edge Crush Test, Application and Reference Guide for Combined Corrugated Board,* Fiber Box Association, Elk Grove Village, IL.

Frank, B. (2003) "Which ECT?," *Corrugated International,* p.3, August.

Frank, B. (2007). "Revisiting clamped ECT," *Corrugated International* 2007; Summer, 7-11.

Gere, J. M., and Timoshenko, S. P. (1972). *Mechanics of Materials,* D. van Nostrand Company, New York.

Haj-Ali, R., Choi, J., Wei, B.-S., Popil, R., and Schaepe, M. (2008). "Refined nonlinear finite element models for corrugated fiberboards/" *Composite Structures* 87(4), 321-333.

Holmes, W. C. (1996). "Holder for corrugated paperboard test specimen during edge compression test," *U.S. Patent* 5,511,432, April 30.

Interface Corporation, Scottsdale, AZ., load cell model LBS-25.

Kellicutt, K. Q., and Landt, D. F. (1951). "Safe stacking life of corrugated boxes," *Fiber Containers* 36(9), 28-38.

Koning, J. W. (1975). "Compressive properties of linerboard as related to corrugated fiberboard containers: A theoretical model," *Tappi Journal* 58(12), 105-108.

Koning, J. W. (1978). "Compressive properties of linerboard as related to corrugated fiberboard containers - Theoretical model verification," *Tappi Journal* 61(8), 69-71.

Koning, J. W. (1986). "New rapid method for determining edgewise compressive strength of corrugated fiberboard," *Tappi Journal* 69(1), 74-76.

Kroeschell, W. O. (1992). "The edge crush test," *Tappi Journal* 75(10),79-82.

Lorentzen and Wettre, Kista, Sweden, Neck Down Cutter Model 110.

McKee, R. C., Gander, J. W., and Wachuta, J. R. (1963). "Compression strength formula for corrugated boxes," *Paperboard Packaging* 48(8), 149-159.

McKee, R. C., Gander, J. W., and Wachuta, J. R. (1961). "Edgewise compression strength of corrugated board," *Paperboard Packaging* 46(11),70-76.

McLain, T. E., and Boitnott, R. L. (1982). "Crush tests rely on parallel-to-flute loading," *Tappi Journal* 65(3), 148-149.

Moody, R. C., and Koning, J. W. (1966). "Effect of loading rate on the edgewise compressive strength of corrugated fiberboard," USDA Research Note FPL-1212, April.

Nordman, L., Kolhonen, E., and Toroi, M. (1978). "Investigation of the compression of corrugated board," *Paperboard Packaging* 63(10), 48-62.

Nordstrand, T. M. (1995). "Parametric study of the post-buckling strength of structural core sandwich panels," *Composite Structures* 30(4), 441-451.

Plantema, F. J. (1966). *Sandwich Construction, The Bending and Buckling of Sandwich Beams, Plates and Shells,* John Wiley and Sons.

Popil, R. E., Coffin, D. W., and Kaewmanee, P. (2004). "The role of interflute buckling on the edgewise compressive strength of corrugated board," *2004 Progress in Paper Physics Seminar, Trondheim Norway.*

Popil, R. E. (2005). "ECT literature review," *TAPPI 2005 Corrugated Packaging Conference, September 26-27, Las Vegas, Nevada.*

Popil, R. E., and Schaepe, M. (2005). "Comparative evaluation of the potential for wax-alternative packaging coatings," *Tappi Journal* 4(8), 25-31.

Popil, R. E., Schaepe, M. K., Haj-Ali, R., Wei, B.-S., and Choi, J. (2006). "Adhesive level effect of corrugated board strength – Experiment and FE modeling," *2006 International Progress in Paper Physics Seminar, Miami University, Oxford Ohio.*

Popil, R. E. (2007). "Shear measurement of board crushing effects," *Paperboard Packaging* 92(7), 37.

Popil, R. E., Coffin, D. W., and Habeger, C. C. (2008). "Transverse shear stiffness and its significance in corrugated board," *Appita Journal* 61(4), 307-312.

Popil, R. E., and Hojjatie, B. (2010). "Effects of component properties and orientation on corrugated container endurance," *Packaging Technology and Science* 23(4), 189-202.

Schaepe, M., and Popil, R. (2006). "A connection between lightweights and ECT strength," *Corrugated International*, September, pg. 3.

Schrampfer, K. E., and Whitsitt, W. J. (1988). "Clamped specimen testing: A faster edgewise crush procedure," *Tappi Journal* 71(10),65-69.

Seth, R. S. (1985). "Relationship between edgewise compressive strength of corrugated board and its components," *Tappi Journal* 68(3), 98-101.

Shalhorn, P., Ju, S., and Gurnagul, N. (2004). "A model for the short-span compression strength of paperboard," *Nordic Pulp and Paper Research Journal* 19(2), 130-134.

Shallhorn, P., Ju, S., and Gurnagul, N. (2005). "A model for the ring crush test of paperboard," *Journal of Pulp and Paper Science* 31(3), 143-147.

Shick, P. E., and Chari, N. C. S. (1965). "Top-to-bottom compression for double wall corrugated boxes," *Tappi Journal* 48(7), 423-430.

T 839, T 811, and T 838 TAPPI Test Methods, TAPPI Press, Atlanta, GA.

Urbanik, T. J. (1990). "Correcting for instrumentation with corrugated fiberboard edgewise crush theory," *Tappi Journal* 73(10), 263-268.

Urbanik, T. J., Caitlin, A. H., Friedman, D. R., and Lund, R. C. (1994). "Edgewise crush test streamlined by shorter time after waxing," *Tappi Journal* 77(1), 83-86.

Urbanik, T. J. (1997). "Linear and nonlinear material effects on postbuckling strength of corrugated containers," AMD vol. 227, MD vol. 77, 93-99, R. Perkins (ed.), The American Society of Mechanical Engineers, New York.

Urbanik, T. J. (2001). "Effect of corrugated flute shape on fiberboard edgewise crush strength and bending stiffness" *Journal of Pulp and Paper Science* 27(10), 330-335.

Whitsitt, W. J. (1988). "Papermaking factors affecting box properties," *Tappi Journal* 71(12), 163-167.

Whitsitt, W. J. (1982). "Optimization of machine properties for compressive strength: Survey of factors affecting compressive strength," IPC Report, March 15.

Whitsitt, W. J., and Baum, G. A. (1987). "Compressive strength retention during fluting," *Tappi Journal* 70(4), 107-112.

Wilson, C. J., and Frank, B. (2009). "An evaluation of ECT sample height for small flute board grades and Box Manufacturer's Certification compliance," *Tappi Journal* 8(6), 24-28.

Article submitted: April 21, 2010; Peer review completed: June 24, 2010; Revised version accepted: February 24, 2012; Published: February 29, 2012.